Rate-determining mechanisms for the adsorption of gold di-cyanide onto activated carbon

by N.M. Vegter* and R.F. Sandenbergh*

Synopsis

The kinetics of adsorption of gold di-cyanide onto activated carbon has been investigated extensively over the past two decades. These studies have demonstrated that both film and intra-particle mass transfer affect the kinetics. The dominant mechanism of intra-particle mass transfer has not yet been identified. In the work described, surface diffusion and pore diffusion are considered as possible rate-determining mechanisms of intra-particle mass transfer. Mathematical models are described that incorporate film mass transfer and the respective intra-particle mass transfer mechanism with equilibrium described by a Freundlich isotherm. Rate constants of film mass transfer and pore or surface diffusivities were estimated by the fitting of the respective models to experimental carbon adsorption data. The estimated pore diffusivities, after they had been corrected for the porosity and tortuosity of the carbon, were found in most instances to be higher than the molecular diffusivity of dilute gold di-cyanide in aqueous solution. This situation is not physically viable. The surface-diffusion mechanism acting in parallel with the pore-diffusion mechanism is thus responsible for the intra-particle transportation of most of the gold.

Introduction

Adsorption by activated carbon is currently the preferred treatment route for the extraction of gold from cyanide leach liquors. Dissolved gold is loaded onto the carbon, which is subsequently eluted and returned to the adsorption circuit via regeneration. The overall performance of a carbon-in-pulp (CIP) plant depends on the characteristics of the carbon and the effective operation of the adsorption, elution, and regeneration sections. A proper understanding of the processes taking place in these sections is therefore essential to ensure the best overall performance of a CIP plant.

The kinetics of adsorption of gold di-cyanide onto activated carbon has been investigated extensively over the past two decades. From these studies, it has become evident that mass-transfer processes are the rate-determining steps, with both film mass transfer and intra-particle mass transfer playing important roles. As yet the dominant intra-particle mass-transfer mechanism or mechanisms (pore and/or surface diffusion) has not been identified nor confirmed with experimental evidence. Surface diffusion as the dominant intra-particle mass-transfer mechanism seems to be the most popular choice in the studies conducted to date. Little physical proof has been presented to demonstrate that surface diffusion is feasible in the aqueous gold di-cyanide–activated carbon system. It was the aim of the study described here to investigate the intra-particle mass-transfer processes responsible for the observed kinetic behaviour.

Overview of kinetics and modelling of gold di-cyanide sorption onto activated carbon

The rate of gold adsorption, in contrast to the adsorption equilibrium, is not strongly affected by temperature; a number of investigators have reported low activation energies for the adsorption of gold and silver di-cyanide onto activated carbon (Table I). These low values are typical of processes rate-controlled by mass transfer, and indicate fast adsorption reaction kinetics. This implies that local equilibrium exists between gold in solution next to the carbon surface and gold adsorbed onto the carbon surface. This assumption has been applied in most of the kinetic models developed to date.

The importance of the rate of mass transport across the solution film surrounding the carbon particle was demonstrated experimentally by Fleming and Nicol[3], Van Deventer[7,8], Jones and Linge[9], and Zarrouki and Thomas[5], all of whom reported an increase in the rate of uptake of gold with an increase in stirring rate. In contrast to this, Dixon *et al.*[1] and McDougall *et al.*[10] reported no effect and 'a small effect' of solution flow

* *Department of Materials Science and Metallurgical Engineering, University of Pretoria, Pretoria 0002.*

© *The South African Institute of Mining and Metallurgy, 1996.* *SA ISSN 0038–223X/3.00 + 0.00. Paper received Jul. 1995; revised paper received Nov. 1995.*

Table I

Reported apparent activation energies for the adsorption of gold and silver di-cyanide onto activated carbon

Species	*E*, kJ/mol	Reference
$Au(CN)_2^-$	10.9	Dixon *et al.*[1]
	13.8	Cho *et al.*[2]
	10.9	Fleming and Nicol[3]
	8.4	Fuerstenau *et al.*[4]
	17.6	Zarrouki and Thomas[5]
$Ag(CN)_2^-$	8.8	Dixon *et al.*[1]
	10.9	Cho and Pitt[6]

rate through their packed beds of carbon on the rate of adsorption of silver and gold di-cyanide respectively. In batch stirred experiments, Van Deventer[8] and Yapu *et al.*[11] found that, as soon as the carbon particles were fully fluidized, the effect of stirring speed on the rate of adsorption became negligible.

For batch adsorption, McDougall *et al.*[10] and Van Deventer[7,8] reported high initial rates of adsorption, followed by a slow approach to overall equilibrium. Fleming and Nicol[3], Zarrouki and Thomas[5], and Jordi *et al.*[12] used interrupted batch adsorption experiments to demonstrate the importance of both film and intraparticle mass transfer; the rate of gold uptake increased when carbon was re-introduced to the gold-containing solution after it had been removed for a timed period. It was assumed that, during this period, the non-uniform gold distribution inside the carbon could become more uniform, increasing the driving force for adsorption at the outer surface of the carbon particle. Gold distributions inside carbon particles as measured by Vegter[13] were indicative of an intra-particle mass-transfer mechanism; the gold penetrated the carbon from the outside until a uniform distribution was obtained.

Fleming and Nicol[3], Van Deventer[7,8], Zarrouki and Thomas[5], and Yapu *et al.*[11] found the rate of adsorption to be inversely proportional to the diameter of the carbon particles. However, Fuerstenau *et al.*[4] found the rate of adsorption to be inversely proportional to the square of the carbon-particle diameter. These observations are roughly consistent with film mass transfer and/or intra-particle mass transfer as rate-determining steps, as identified above.

The overall rate of gold uptake is influenced by the pH, ionic strength, cation type, and gold concentration in solution[3,4,10]. It is well known that these factors influence the adsorption equilibrium. However, it is not known whether the changes brought about by these factors in the adsorption equilibrium (thus determining the driving force of the rate processes) fully account for the changes in the overall uptake rate.

In an attempt to account for the observed kinetic phenomena discussed here, four mathematical models were developed respectively based on the following rate-determining steps:

(1) the adsorption–desorption reaction
(2) film mass transfer
(3) intra-particle mass transfer by pore diffusion
(4) film and intra-particle mass transfer by surface diffusion.

These models are discussed briefly below.

(1) In the kinetic models based on adsorption–desorption, reaction rate-control Langmuir adsorption kinetics were assumed. Yapu *et al.*[11] proposed a Langmuir–Hinselwood type of rate equation as the rate-controlling mechanism for the adsorption of gold and silver di-cyanide. This is in conflict with the observed effects discussed earlier, which point to mass transfer as controlling the rate of the adsorption process. Carrier *et al.*[14], Stange *et al.*[15], and Woollacott *et al.*[16] used this theory, in modelling the adsorption of gold di-cyanide in plant simulations, for its simplicity rather than its mechanistic validity.

(2) Nicol *et al.*[17] proposed a double-film mass-transfer kinetic model based on linear concentration gradients in the carbon and solution, with assumed local equilibrium between the gold on the carbon and the gold in solution at the outer surface of the carbon. The equilibrium was described by a linear isotherm. Johns[18] and Zarrouki and Thomas[5] proposed a film mass-transfer model with equilibrium given by a Freundlich isotherm. Fuerstenau *et al.*[4] proposed a model that is rate-controlled by solution-film mass transfer, but that neglects the effects of equilibrium. This model is therefore irreversible and applicable only to low gold concentrations on the carbon during the initial period of adsorption.

(3) Cho *et al.*[2] and Cho and Pitt[6] proposed a model based on the diffusion of gold and silver di-cyanide in the pore solution inside the carbon particles. The rate of film mass transfer was neglected. Freundlich isotherms were used to describe the adsorption equilibrium.

(4) Van Deventer[7,8] and Le Roux *et al.*[19] demonstrated the inadequacy of omitting the rate of film mass transfer from the kinetic model. Van Deventer[7,8] proposed two intraparticle mass-transfer mechanisms: diffusion of gold di-cyanide along the macro-pore walls by surface diffusion, followed by transfer from the macro-pores into the micro-pores. This last process accounted for the slow approach to overall equilibrium in batch adsorption. His complete model included film mass transfer of gold di-cyanide, surface diffusion in the macro-pores, and a first-order rate equation for the transfer of gold di-cyanide from the macro-pore into the micro-pores of the carbon granule. The equilibrium was described by a Freundlich isotherm. Le Roux *et al.*[19] proposed a model based on the rate of film mass transfer and surface diffusion into the carbon granule, with the equilibrium described by a Freundlich isotherm. This model, with some modifications, was applied successfully in a number of studies[12,20-25] to describe the adsorption of gold and silver di-cyanide in the presence of fine suspended solids and various organic foulants.

It can be concluded that there is convincing evidence that the overall rate of gold uptake during adsorption is limited both by mass transfer across the solution film surrounding the carbon particle and by diffusion inside the carbon particle; however, there is no substantial agreement on the appropriate mathematical description of this process. In this paper, two kinetic models to describe the situation are considered: (1) film mass transfer and pore diffusion and (2) film mass transfer and surface diffusion. These models were fitted to experimental data as a test of their performance.

Kinetic models

A list of the symbols used is given at the end of the paper.

Given a thermodynamic driving force, the adsorption of gold di-cyanide onto activated carbon may take place in a number of sequential and/or parallel transport and reaction steps. These rate steps include the following:

(1) mass transport of gold di-cyanide and cations across the solution film surrounding the carbon particle
(2) transport by pore diffusion of the dissolved species, in the solution filling the pores
(3) the sorption reaction
(4) transport by surface diffusion of the adsorbed gold di-cyanide along the pore walls.

Given the ample evidence as presented earlier that the sorption process is under mass-transfer rate control, the rate of the sorption reaction was neglected in the development of the model.

A single-component Freundlich isotherm was used in the present study to describe the equilibrium between solution species and adsorbed species. The Freundlich isotherm is given by

$$q_{eq} = B_F C_{eq}^b, \qquad [1]$$

with q_{eq} and C_{eq} the equilibrium gold concentrations on the carbon and in the solution respectively, and B_F and b the Freundlich pre-exponent and exponent respectively.

The carbon particle was assumed to be either spherical or cylindrical with an outer radius of r_s. It was assumed, for cylindrically shaped particles, that the end effects could be neglected. The rate of mass transfer of gold across the stagnant film surrounding the carbon particle is given by

$$J_f = -k_f\left[C_b - C(r_s)\right], \quad r = r_s, \qquad [2]$$

with C_b the bulk solution concentration of gold and k_f the film mass-transfer rate constant. The rate of mass transfer inside the carbon particle due to diffusion of the adsorbed gold species along the surfaces of the pore walls is given by

$$J_s = -\rho_p D_s \frac{\partial q}{\partial r}, \quad 0 \le r \le r_s, \qquad [3]$$

with ρ_p the density of the carbon, and D_s the effective surface diffusivity. The rate of mass transfer inside the carbon particle due to diffusion of the gold in the pore solution is given by

$$J_p = -D_p \frac{\partial C}{\partial r}, \quad 0 \le r \le r_s, \qquad [4]$$

with D_p the effective pore diffusivity. At any position within a carbon particle, the mass balance of gold in pore solution and that adsorbed onto the carbon is given by

$$\rho_p \frac{\partial q}{\partial t} + \varepsilon_p \frac{\partial C}{\partial t} = \frac{D_p}{r^i}\frac{\partial}{\partial r}\left(r^i \frac{\partial C}{\partial r}\right) + \frac{D_s \rho_p}{r^i}\frac{\partial}{\partial r}\left(r^i \frac{\partial q}{\partial r}\right), \quad 0 \le r \le r_s, \qquad [5]$$

with ε_p the porosity and i equal to 0, 1, or 2 for slab-, cylindrical-, or spherical-shaped particles respectively.

The boundary and initial conditions are based on the following assumptions.

(1) The diffusion and sorption processes take place symmetrically inside the carbon particle:

$$r = 0: \quad \frac{\partial C}{\partial r} = \frac{\partial q}{\partial r} = 0. \qquad [6]$$

(2) The fluxes of species due to surface diffusion and pore diffusion equal the flux due to film mass transfer at the outer surface:

$$r = r_s: \quad k_f\left[C_b - C(r_s)\right] = D_p \frac{\partial C}{\partial r} + D_s \rho_p \frac{\partial q}{\partial r}. \qquad [7]$$

(3) Uniform concentrations with no gold in the pore solution or adsorbed onto the carbon existed at the start of the experiment:

$$t = 0: \quad \bar{C} = C(r) = q(r) = \bar{q} = 0, \quad 0 \le r \le r_s. \qquad [8]$$

The initial concentration of gold in the bulk solution is given by

$$t = 0: \quad C_b = C_{b0}. \qquad [9]$$

The mean concentrations of gold adsorbed onto the carbon particle and in the pore solution inside the carbon particle are given by

$$\bar{q} = \frac{i+1}{r_s^{i+1}} \int_0^{r_s} q\, r^i dr, \qquad [10]$$

$$\bar{C} = \frac{i+1}{r_s^{i+1}} \int_0^{r_s} C\, r^i dr. \qquad [11]$$

Depending on the type of reactor in which the sorption process takes place, a suitable gold balance equation can be derived. The experiments for this study were all performed in batch reactors. If the characteristics of all the carbon particles are uniform, the mass balance of gold in the batch reactor is given by

$$-V\frac{dC_b}{dt} = m\frac{d\bar{q}}{dt} + \frac{m\varepsilon_p}{\rho_p}\frac{d\bar{C}}{dt}, \qquad [12]$$

with m the mass of carbon and V the volume of solution. Integration of eq. [12] subject to the initial conditions listed in eqs. [8] to [9] yields

$$C_b = C_{b0} - \frac{m}{V}\bar{q} + \frac{m\varepsilon_p}{V\rho_p}\bar{C}. \qquad [13]$$

Rate determined by film mass transfer and pore diffusion

If film and pore diffusion are rate limiting, the implication is that pore diffusion is significantly faster than surface diffusion because these processes take place in parallel. If the gold concentration in solution is low compared with a high concentration on the carbon, as is normally the case with commercial adsorbers, the second term on the left-hand side of eq. [5] is negligibly small, as are the last terms of eqs. [12] and [13]. A complication under these conditions is that the slope of the Freundlich isotherm tends to infinity as the concentration of gold in solution approaches zero. In the present work, to permit the numerical solution of the set of equations, the Freundlich isotherm was approximated by a

Langmuir isotherm at dilute concentrations. At an arbitrarily chosen dilute concentration, C_d and q_d, the Langmuir isotherm constants were calculated so that the slopes of the Freundlich and Langmuir isotherms coincided. The Langmuir parameters are given by

$$B_{L\,d} = \frac{1-b}{b\,C_d}, \qquad [14]$$

$$q_d^* = B_F C_d^b \left(\frac{b}{1-b}+1\right), \qquad [15]$$

with q_d^* and $B_{L\,d}$ the Langmuir isotherm parameters in terms of the Freundlich isotherm parameters. The equilibrium is thus described by the following two equations:

$$q = \frac{q_d^* B_{L\,d} C}{1+B_{L\,d} C}, \quad 0 \le C \le C_d, \qquad [16]$$

$$q = B_F C^b, \quad C \ge C_d. \qquad [17]$$

Application of the stated assumptions reduces eqs. [5] and [10] to

$$C > C_d: \ \rho_p B_F b\, C^{b-1} \frac{\partial C}{\partial t} = D_p\, r^{-i} \frac{\partial}{\partial r}\left(r^i \frac{\partial C}{\partial r}\right), \quad r_d < r \le r_s, \qquad [18]$$

$$C \le C_d: \ \frac{\rho_p B_F C_d^{b-1} b}{\left[b+(1-b)\,C/C_d\right]^2} \frac{\partial C}{\partial t} = D_p\, r^{-i} \frac{\partial}{\partial r}\left(r^i \frac{\partial C}{\partial r}\right), \quad 0 \le r \le r_d, \qquad [19]$$

$$\bar{q} = \frac{i+1}{r_s^{i+1}}\left[\int_0^{r_d} \frac{B_F C_d^{b-1} C}{b+(1-b)\,C/C_d} r^i dr + \int_{r_d}^{r_s} B_F C^b r^i dr\right], \qquad [20]$$

with r_d the radius at which the transition from the approximate Langmuir to the Freundlich isotherm takes place. The following non-dimensional variables are defined:

$$Q = \frac{q}{B_F C_{b0}^b}, \quad \varsigma = \frac{C}{C_{b0}}, \quad X = \frac{r}{r_s}, \quad \alpha = \frac{m B_F C_{b0}^b}{V C_{b0}}, \qquad [21]$$

$$\tau_p = \frac{D_p C_{b0}\, t}{\rho_p\, b\, B_F\, C_{b0}^b\, r_s^2}, \quad Bi_p = \frac{k_f r_s}{D_p}. \qquad [22]$$

These allow the conversion of eqs. [6] to [9], [13], and [18] to [20] to non-dimensional form:

$$\varsigma > \varsigma_d: \ \varsigma^{b-1} \frac{\partial \varsigma}{\partial \tau_p} = \frac{1}{X^i} \frac{\partial}{\partial X}\left(X^i \frac{\partial \varsigma}{\partial X}\right), \quad X_d \le X \le 1, \ \tau_p > 0, \qquad [23]$$

$$\varsigma \le \varsigma_d: \ \frac{\varsigma_d^{b-1}}{\left[b+(1-b)\varsigma/\varsigma_d\right]^2} \frac{\partial \varsigma}{\partial \tau_p} = \frac{1}{X^i} \frac{\partial}{\partial X}\left(X^i \frac{\partial \varsigma}{\partial X}\right), \quad 0 \le X \le X_d, \qquad [24]$$

$$\frac{\partial \varsigma}{\partial X} = 0, \quad X = 0, \quad \tau_p \ge 0, \qquad [25]$$

$$\frac{\partial \varsigma}{\partial X} = Bi_p\left[\varsigma_b - \varsigma(1)\right], \quad X = 1, \ \tau_p > 0, \qquad [26]$$

$$\bar{Q} = (i+1)\left[\int_0^{X_d} \frac{\varsigma_d^{b-1} \varsigma X^i}{b+(1-b)\varsigma/\varsigma_d} dX + \int_{X_d}^{1} \varsigma^b X^i dX\right], \qquad [27]$$

$$\varsigma_b = 1-\alpha\,\bar{Q}, \qquad [28]$$

$$\tau_p = 0: \ \varsigma_b = 1, \ \varsigma(X) = 0, \ 0 \le X \le 1, \qquad [29]$$

with X_d the radius at which the transition between the Langmuir and the Freundlich isotherms occurs.

Rate determined by film mass transfer and surface diffusion

If film and surface diffusion are rate limiting, the assumptions applied to the general model are similar to those already postulated. The following non-dimensional variables are defined:

$$\tau_s = \frac{D_s t}{r_s^2}, \quad Bi_s = \frac{k_f C_{b0} r_s}{D_s \rho_p B_F C_{b0}^b}. \qquad [30]$$

By use of the non-dimensional variables defined in eqs. [22] and [30], eqs. [5] to [10] and [13] are converted to non-dimensional form as follows:

$$\frac{\partial Q}{\partial \tau_s} = \frac{1}{X^i} \frac{\partial}{\partial X}\left(X^i \frac{\partial Q}{\partial X}\right), \quad 0 \le X \le 1, \ \tau_s > 0, \qquad [31]$$

$$\frac{\partial Q}{\partial X} = 0, \quad X = 0, \quad \tau_s \ge 0, \qquad [32]$$

$$\frac{\partial Q}{\partial X} = Bi_s\left[\varsigma_b - Q^{1/b}(1)\right], \quad X = 1, \ \tau_s > 0, \qquad [33]$$

$$\bar{Q} = (i+1)\int_0^1 Q\, X^i\, dX, \qquad [34]$$

$$\varsigma_b = 1-\alpha\,\bar{Q}, \qquad [35]$$

$$\tau_s = 0: \ \varsigma_b = 1, \ \bar{Q} = Q(X) = 0, \ 0 \le X \le 1. \qquad [36]$$

Numerical solution of the model equations

The partial-differential equations of the two models rate-limited by film and intra-particle mass transfer (eqs. [21] to [29] and [31] to [36] respectively) were solved with the NAG D03PGF routine[26], which is based on the method of lines and Gear's method. The mean concentrations of gold inside the carbon particles (eqs. [27] and [34]) were obtained by the fitting of a cubic spline function according to the IMSL DSCINT routine[27] and integration of the resulting function with the IMSL DCSITG routine[27].

Experimental procedure

Batch equilibrium and kinetic experiments were performed with 0.2 M KOH aqueous solutions containing initial concentrations of gold in solution of 10 to 2000 mg/l at 30, 50, 70, and 90°C respectively.

Material

The experimental work was conducted with particles of Norit RB3 cylindrical peat carbon. The diameters of the carbon cylinders were 2.8 mm, and the lengths varied between 7 and 10 mm. The carbon was prepared for the experiments by repeated boiling and washing in distilled water, after which it was stored in distilled water. Distilled water and reagent-grade chemicals were used in all the experiments.

Equilibrium and kinetic batch experiments

Weighed amounts of wet, washed activated carbon were contacted with measured volumes of 0.2M KOH solutions spiked with gold as $KAu(CN)_2$. All the experiments were conducted in closed glass reaction vessels having a volume of 2.5 litres and being equipped with four baffles. These were equipped with condensers to limit evaporation losses at 70 and 90°C. Stirring was conducted with a flat 316 stainless-steel four-bladed paddle at a controlled and recorded rate by a Heidolph overhead stirrer. At at stirring rate of 100 r/min, the carbon particles moved along the bottom; at 400 r/min, the particles were fully suspended in the reactor. Samples of the solution in volumes of 20 ml were taken for gold analysis at timed intervals. The final volume of the solution and the dry mass of the carbon (after overnight drying at 120°C) were determined and recorded. The temperature was controlled by a thermostatted water bath at 30, 50, 70, and 90°C for the respective experiments. Care was taken to equilibrate the temperatures of the solution before the start of the kinetic experiments. The equilibrium experiments were performed in sealed bottles with contact times of two weeks. The samples of solution were analysed for gold by inductively coupled plasma atomic-emission spectroscopy and/or atomic-absorption spectroscopy. The final gold concentrations on the carbon were determined by fire assay.

The bulk equilibrium parameters were obtained by the fitting of the Freundlich relationship to the equilibrium gold concentrations in solution and on the carbon as determined in the batch experiments. These data sets and equilibrium relationships were transformed to linear format, and the parameters were estimated by linear regression.

For a given set of rate parameters (such as film and pore or surface diffusivities), the kinetic models can be solved numerically to yield the model-calculated bulk gold concentration in the solution with time. The measured bulk gold concentrations in the solutions, $C_{exp(t_n)}$, can be compared with those calculated from the model, $C_{mod(t_n)}$, in the following object function:

$$\sigma^2 = \frac{1}{C_{b0}^2 (N-K-1)} \sum_{n=1}^{N} \left[C_{\mathrm{mod}}(t_n) - C_{\exp}(t_n) \right]^2, \quad [37]$$

with K the number of parameters estimated, t_n the time of the n-th timed sample, and N the total number of timed samples. The optimal rate parameters for the object function were searched by use of the IMSL DBCPOL routine[27], which is based on the complex method. Widely varying rate parameters for essentially the same experimental conditions (other than the initial gold concentration) were obtained for the data sets of Van der Merwe[28] and Van Deventer[29] with this method. As the stirring conditions were kept constant for a given experimental campaign, the average film mass-transfer coefficient for each campaign was estimated from the data sets for the initial rate. The initial rate of adsorption is given by

$$\left.\frac{dC_b}{dt}\right|_{t=0} = -\frac{(i+1)\, m\, C_{b0}}{\rho_p r_s V} k_f. \quad [38]$$

The pore and surface diffusivity were in these instances estimated by the optimization of eq. [37] via a line search technique.

Results and discussion

Equilibrium

The adsorption equilibrium becomes less favourable with increasing temperature, as demonstrated by McDougall *et al.*[10]. Their findings were confirmed by the similar findings of Van der Merwe[28] and by the present study (Figure 1 and Table II). The carbon particles in contact with solutions having final gold concentrations of more than 350 mg/l in the adsorption experiments at 70 and 90°C turned yellowish, indicating the plating of elemental gold. The absence of free cyanide, the high gold concentrations, and the high temperatures resulted in the instability of the gold di-cyanide complex and subsequent plating of gold. In these instances, cyanide would be required to achieve complete elution. The kinetic experiments in the present study were conducted at low gold concentrations at which the contribution of the plating mechanism had been assumed to be less important.

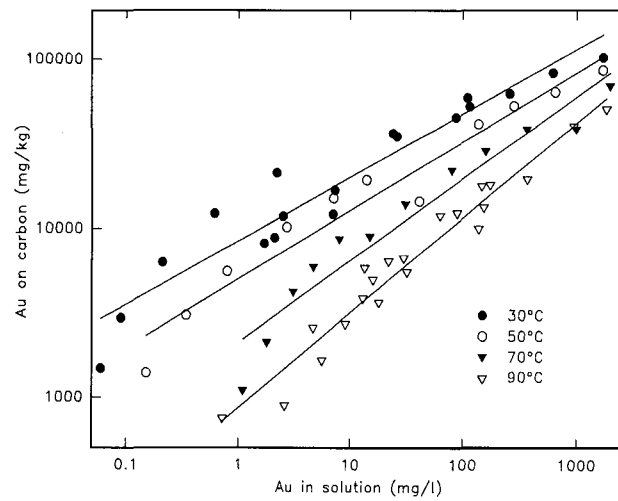

Figure 1—Adsorption equilibrium of gold on Norit RB3 activated carbon in 0.2M KOH at different temperatures

Table II

Freundlich isotherm parameters for the adsorption of gold onto Norit RB3 activated carbon in 0.2 M KOH aqueous solution

T °C	B_F mg^{1-b}.l^b/kg	b	r^2
30	8 472.8	0.379	0.93
50	5 033.3	0.409	0.95
70	2 121.0	0.487	0.93
90	872.0	0.564	0.96

Intra-particle mass transfer as rate-controlling mechanism

In previous studies, the rate of adsorption was shown to be fairly insensitive to temperature. From this it was inferred that the sorption reaction was not rate determining. Intra-particle mass transfer was shown to be important, but the question remained: which intra-particle mechanism? Three mechanisms were proposed:

(1) diffusion in the pore solution
(2) surface diffusion along the pore walls
(3) surface diffusion along the macro-pore walls and transfer from the macro-pores into the micro-pores.

These mechanisms can be tested by evaluation of the respective models fitted to the experimental data, each mechanism being assumed in turn. A test for the proposal that diffusion in the pore solution is the dominant intra-particle mechanism involves the value of the pore diffusivity, which is obtained from the fitting of the relevant model to the experimental data. Once this estimated pore diffusivity has been corrected for the porosity and tortuosity of the carbon, it can be compared with the reported diffusivity of dilute gold di-cyanide in aqueous solution. If the fitted model is correct, these values should be similar. For the surface-diffusion mechanisms with and without transfer from the macro- to the micro-pores, no comparative constants are available. Discrimination between these latter two mechanisms would be possible only if based on the goodness of fit of each model.

In this work, mechanisms (1) and (2), as the simplest mechanisms that can feasibly be active, were fitted to data from Van der Merwe[28], Van Deventer[29], and Le Roux[30], together with experimental data from the present study. The parameters and experimental conditions for these data sets are listed in Table III. The estimated constants for the film mass-transfer rate, and the effective pore and surface diffusivities for the respective models, are given in Tables IV to VIII. The experimental data and the fitted models are shown in Figures 2 to 7. It is evident that the rate-controlling mechanism(s) cannot be identified solely from the quality of the model fit; both mechanisms (1) and (2) provide satisfactory fits.

Table III

Parameters used to fit the models to the data sets

Reference	Le Roux[30]	Van Deventer[29]		Van der Merwe[28]	Present work
Carbon type	G210 AS	G210 AS (batch A)	G210 AS (batch B)	Beatrix Gold Mine	Norit RB3
Temperature	20°C	20°C	20°C	20°C	Figure 7
pH	–	8.5	8.5	7.0	–
CN^- (M)	0.004	–	–	–	–
OH^- (M)	0.044	–	–	–	0.2
Stirring rate (r/min)	250	240	150	1350	Table VIII
B_F (mg^{1-b}·m^{3b}/kg)	1880	26669	29843	7693	Table II
b	0.393	0.0907	0.075	0.204	Table II
m (g)	0.5	2.0	2.0	Table VII	2.65
ρ (kg·m^{-3})	818	980	980	838	574
r_s (mm)	0.775	0.92	0.775	0.71	1.4
V (litre)	2.0	2.0	2.0	1.5	2.0

Table IV

Estimated rate parameters for the film-and-pore-diffusion model and the film-and-surface-diffusion model fitted to Le Roux's[30] experimental data

C_{b0} mg/l	k_f m/s	D_p m^2/s	D_s m^2/s	Bi	σ^2
5.3	1.80 x 10^{-4}	5.80 x 10^{-9}	–	24.0	4.1 x 10^{-4}
8.7	1.40 x 10^{-4}	4.73 x 10^{-9}	–	23.0	2.7 x 10^{-4}
12.5	1.67 x 10^{-4}	7.61 x 10^{-9}	–	17.0	1.4 x 10^{-3}
32.0	1.03 x 10^{-4}	9.36 x 10^{-9}	–	8.5	1.9 x 10^{-4}
54.4	1.03 x 10^{-4}	9.36 x 10^{-9}	–	8.5	2.5 x 10^{-4}
111.1	1.92 x 10^{-4}	4.56 x 10^{-9}	–	32.7	3.5 x 10^{-4}
5.3	8.27 x 10^{-5}	–	6.45 x 10^{-13}	11.7	7.4 x 10^{-4}
8.7	5.46 x 10^{-5}	–	8.75 x 10^{-13}	7.8	1.4 x 10^{-4}
12.5	7.18 x 10^{-5}	–	1.18 x 10^{-12}	9.4	1.6 x 10^{-3}
32.0	6.88 x 10^{-5}	–	2.26 x 10^{-12}	8.3	2.2 x 10^{-4}
54.4	8.94 x 10^{-5}	–	2.93 x 10^{-12}	11.5	1.9 x 10^{-4}
111.1	6.92 x 10^{-4}	–	2.84 x 10^{-12}	141.5	4.0 x 10^{-4}

Table V

Estimated rate parameters for the film-and-pore-diffusion model and the film-and-surface-diffusion model fitted to Van Deventer's experimental data[29], carbon batch A with k_f = 3.31 x 10^{-5} m/s

C_{b0} mg/l	D_p m^2/s	D_s m^2/s	Bi	σ^2
25	4.00 x 10^{-8}	–	0.76	9.8 x 10^{-3}
50	5.10 x 10^{-9}	–	5.96	1.0 x 10^{-2}
100	6.25 x 10^{-10}	–	48.7	5.5 x 10^{-3}
25	–	4.80 x 10^{-12}	2.42	9.4 x 10^{-3}
50	–	5.24 x 10^{-13}	41.7	2.5 x 10^{-3}
100	–	4.62 x 10^{-13}	88.7	1.2 x 10^{-3}

Table VI

Estimated rate parameters for the film-and-pore-diffusion model and the film-and-surface-diffusion model fitted to Van Deventer's experimental data[29], carbon batch B with k_f = 6.4 x 10^{-5} m/s

C_{b0} mg/l	D_p m^2/s	D_s m^2/s	Bi	σ^2
25	3.83 x 10^{-8}	–	1.29	3.0 x 10^{-2}
50	8.00 x 10^{-10}	–	61.7	2.2 x 10^{-2}
75	1.50 x 10^{-9}	–	32.9	3.9 x 10^{-3}
100	6.46 x 10^{-10}	–	76.4	6.6 x 10^{-3}
25	–	5.82 x 10^{-13}	33.9	2.4 x 10^{-3}
50	–	2.82 x 10^{-13}	133.0	8.8 x 10^{-3}
75	–	2.32 x 10^{-13}	235.0	3.6 x 10^{-3}
100	–	2.30 x 10^{-13}	309.7	2.9 x 10^{-3}

Table VII

Estimated rate parameters for the film-and-pore-diffusion model and the film-and-surface-diffusion model fitted to Van der Merwe's experimental data[28], with k_f = 1.11 x 10^{-5} m/s

C_{bo} mg/l	m g	D_p m^2/s	D_s m^2/s	Bi	σ^2
11.4	1.5	2.74 x 10^{-10}	–	28.7	5.5 x 10^{-4}
11.4	0.7	5.25 x 10^{-10}	–	15.0	2.3 x 10^{-3}
20.1	1.0	6.56 x 10^{-10}	–	12.0	1.6 x 10^{-3}
20.1	0.5	3.05 x 10^{-10}	–	2.6	3.3 x 10^{-3}
11.4	1.5	–	8.01 x 10^{-14}	40.6	1.3 x 10^{-4}
11.4	0.7	–	7.87 x 10^{-14}	41.3	2.6 x 10^{-4}
20.1	1.0	–	5.87 x 10^{-14}	35.2	3.3 x 10^{-4}
20.1	0.5	–	5.35 x 10^{-14}	38.7	2.9 x 10^{-4}

Table VIII

Estimated rate parameters for the film-and-pore-diffusion model and the film-and-surface-diffusion model for the adsorption of gold di-cyanide onto Norit RB3 carbon

	k_f m/s	D_p m^2/s	D_s m^2/s	Bi	σ^2
30°C,					
100 r/min	3.38 x 10^{-5}	5.21 x 10^{-9}	–	9.1	4.0 x 10^{-3}
200 r/min	5.74 x 10^{-5}	9.77 x 10^{-9}	–	8.2	7.2 x 10^{-4}
400 r/min	7.21 x 10^{-5}	9.64 x 10^{-9}	–	10.5	1.9 x 10^{-3}
30°C,					
100 r/min	2.17 x 10^{-5}	–	4.47 x 10^{-12}	8.9	2.1 x 10^{-3}
200 r/min	5.69 x 10^{-5}	–	7.92 x 10^{-12}	13.4	4.4 x 10^{-4}
400 r/min	4.75 x 10^{-3}	–	6.48 x 10^{-12}	1376	3.3 x 10^{-3}
200 r/min					
50°C	1.54 x 10^{-4}	–	1.12 x 10^{-11}	39.7	2.6 x 10^{-3}
70°C	9.95 x 10^{-3}	–	2.41 x 10^{-11}	2228	4.3 x 10^{-3}
90°C	9.66 x 10^{-3}	–	4.06 x 10^{-11}	2455	2.2 x 10^{-3}

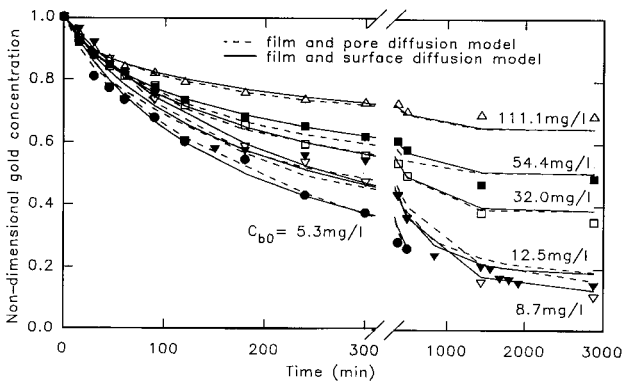

Figure 2—Film-and-pore-diffusion model and film-and-surface-diffusion model fitted to Le Roux's experimental data[30]

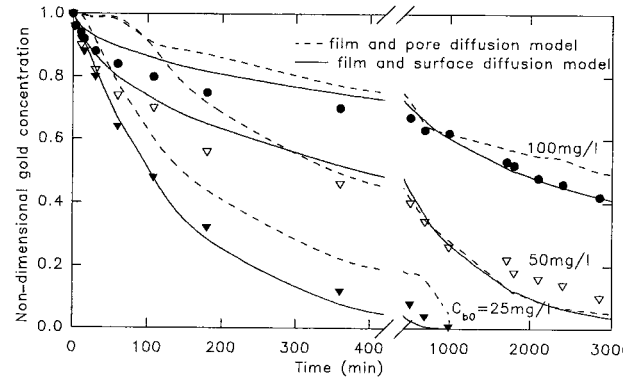

Figure 3—Film-and-pore-diffusion model and film-and-surface-diffusion model fitted to Van Deventer's experimental data[29], carbon batch A

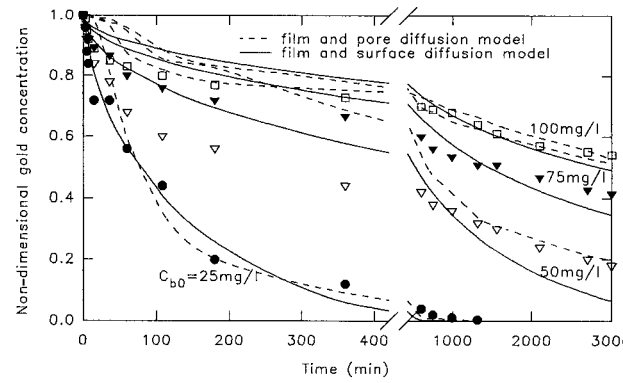

Figure 4—Film-and-pore-diffusion model and film-and-surface-diffusion model fitted to Van Deventers's experimental data[29], carbon batch B

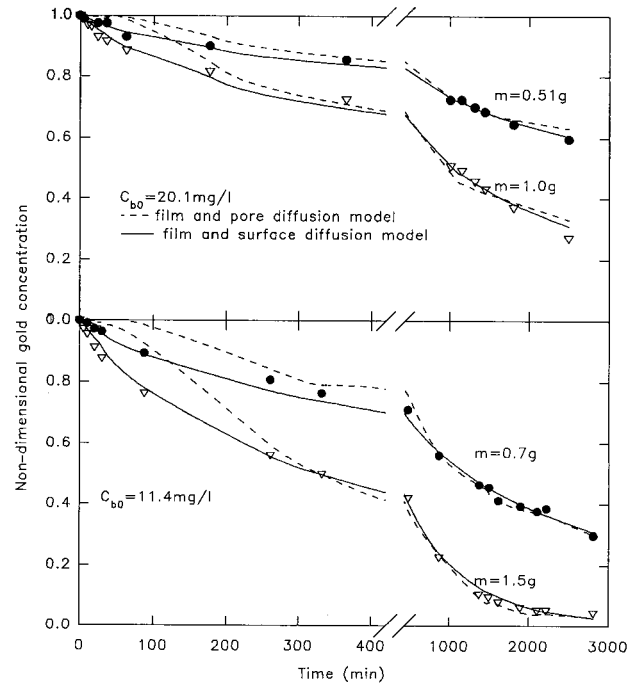

Figure 5—Film-and-pore-diffusion model and film-and-surface-diffusion model fitted to Van der Merwe's experimental data[28]

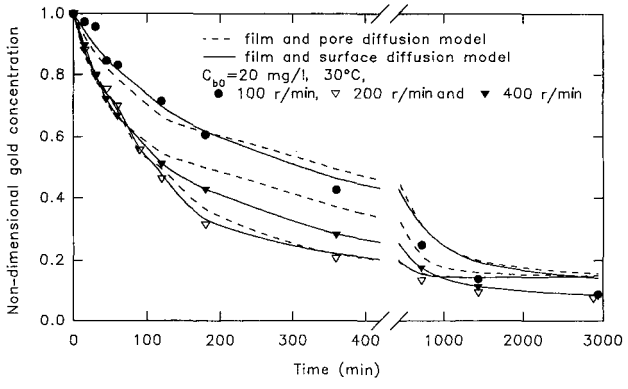

Figure 6—Film-and-pore-diffusion model and film-and-surface-diffusion model fitted to the adsorption behaviour of Norit RB3 carbon under different stirring conditions

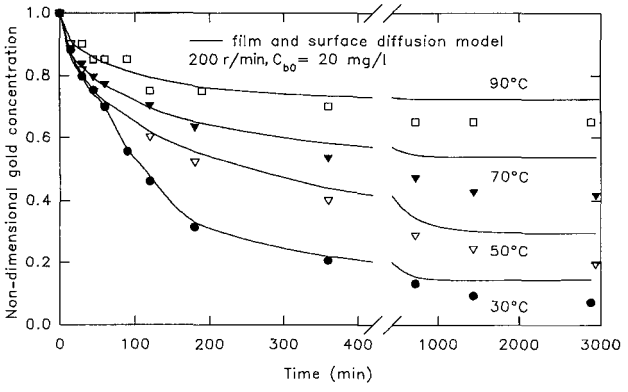

Figure 7—Effect of temperature on the adsorption behaviour of gold di-cyanide onto Norit RB3 carbon from 0.2M KOH solution

For the film-and-pore-diffusion model to be mechanistically valid, the estimated effective pore diffusivities should be equal to the theoretical possible effective pore diffusivity. They should also be smaller than the molecular diffusivity of gold di-cyanide in solution because the theoretical effective pore diffusivity, D_p, is given by

$$D_p = \varepsilon_p D/\tau_m, \quad [39]$$

with D the molecular diffusivity of the species in solution, and τ_m the tortuosity of the porous structure. The porosity of activated carbon varies[31,32] between 0.45 and 0.69. Leyva-Ramos and Geankoplis[32] have listed the tortuosities for different activated carbons as varying between 1.7 and 16, with values of around 3 the most frequent. The molecular diffusivity of gold di-cyanide complex in aqueous cyanide solution has been measured in several gold-electroplating studies by different investigators (Table IX). The estimated effective pore diffusivities in the present work should thus have values between 4.0×10^{-10} and 3.0×10^{-11} m²/s for the film-and-pore-diffusion model to be mechanistically valid.

From Tables IV to VIII it is evident that the estimated effective pore diffusivities were in most instances higher than the theoretical effective pore diffusivity based on the molecular diffusivity of gold di-cyanide in solution. This means that, if the only available mechanism was pore diffusion, the measured gold flux was greater than the maximum theoretical flux. This indicates that another mechanism, surface diffusion, which acts in parallel with pore diffusion, contributed the difference between these two fluxes. In most instances, the estimated effective pore diffusivities were orders of magnitude greater than the theoretical pore diffusivity; most of the gold was thus transported by surface diffusion.

Table IX

Reported molecular diffusivity of gold di-cyanide in aqueous solutions

D m²/s	Conditions	Reference
1.68×10^{-9}	35 g/l KCN, 60°C	Cheh[33]
1.8×10^{-9}	0.2M KOH, 0.2M KCN, 61°C	MacArthur[34]
1.0×10^{-9}	0.01M NaCN, 0.02M NaCl, 21°C	Nicol *et al.*[35]
1.25×10^{-9}	0.01M NaCN, 25°C	Rubcumintara and Han[36]

The adsorption behaviour reported by Van der Merwe[28], and subsequently also the estimated rate parameters, were notably different from those in other studies. His values for the estimated pore diffusivities (Table VII) indicate that pore diffusion may be rate determining. The carbon used in that study originated from the CIP circuit of Beatrix Gold Mine, and magnetic stirring at a high rate was employed. All the carbons used in the other studies were new, and the stirring was relatively slow, being carried out with an overhead impeller. The noted difference in behaviour may thus be due to (1) modification of the carbon by fouling and/or repeated regeneration during its industrial use, and/or (2) the stirring mechanism employed.

The values of the estimated surface diffusivities of the coconut-derived carbons used by Van der Merwe[28], Le Roux[30], and Van Deventer[29] varied between 5×10^{-14} and 5×10^{-12} m²/s. The same type of carbon from the same supplier was used by Le Roux and Van Deventer. The variation in their findings may be attributed, to some extent, to variation in the properties of the carbon. The estimated surface diffusivities at 30°C on the peat-derived Norit carbon varied between 4.5×10^{-12} and 7.9×10^{-12} m²/s.

The quality of the model fit was not satisfactory in all cases, and may have been affected by

(1) the validity of the model assumptions
(2) the accuracy of the predicted isotherm
(3) the accuracy of the concentration measurements at the timed intervals.

As equilibrium is approached, all the models are constrained by the mass balance. Errors in the equilibrium prediction and/or experimental measurements will be most evident as overall equilibrium is approached. To improve the quality of model fit, additional mechanisms can be incorporated in the models; unfortunately, the physical validity of these mechanisms is often impossible to test. Both Van Deventer[29] and Van der Merwe[28] applied more complex models to obtain a better correspondence between their models and experimental data.

Effect of film mass transfer

The values of the estimated modified Biot numbers for the film-and-surface-diffusion model varied over a wide range for the various data sets. In most instances, the Biot numbers

were larger than 1, indicating that intra-particle mass transfer would be a rate-determining step. The very large Biot numbers obtained for Van Deventer's data[29] may indicate that intra-particle mass transfer was the only rate-determining step. However, these model fits were not satisfactory and necessitated the development of the more complex kinetic model proposed by Van Deventer[7,8].

Most of the estimated film mass-transfer coefficients varied between 10^{-5} and 10^{-4} m/s. These values are of the same magnitude as those reported by Harriot[37].

The rate of gold uptake increased with increasing stirring speed at 30°C (Figure 6). This confirms similar earlier findings reported of Nicol *et al.*[17], Van Deventer[7,8], and Zarrouki and Thomas[5]. These findings affirm that film mass transfer is one of the rate-determining steps in the adsorption of gold di-cyanide onto activated carbon.

Effect of temperature on the rate of adsorption

McDougall *et al.*[10] observed that the rate of gold adsorption increased with increasing temperature, but that the extraction decreased owing to the less favourable adsorption isotherm. These findings are confirmed by the present results (Figures 1 and 7). An apparent activation energy of 25.8 kJ/mol was calculated for the surface diffusivity of gold di-cyanide onto Norit RB3 carbon (Figure 8). The modified Biot numbers increased substantially with increasing temperature (Table VIII). This indicates that surface diffusion becomes the dominant rate-determining process with increasing temperature.

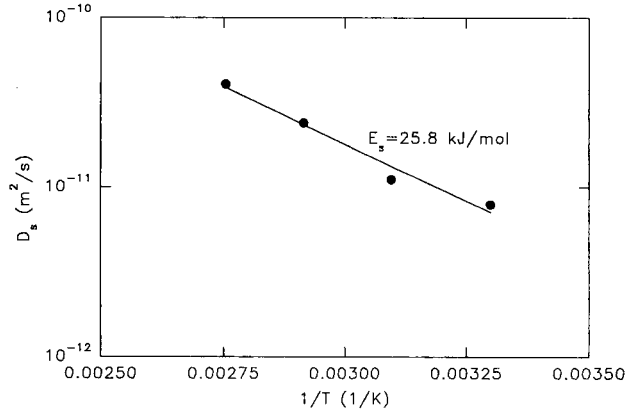

Figure 8—Arrhenius plots of estimated surface diffusivities for the adsorption of gold di-cyanide onto Norit RB3 carbon from 0.2M KOH solution

Conclusion

Surface diffusion and pore diffusion were considered as possible rate-determining mechanisms in intra-particle mass transfer. In most instances, the estimated pore diffusivities were orders of magnitude higher than the molecular diffusivity of dilute gold di-cyanide in aqueous solution after they had been corrected for porosity and tortuosity. Because this situation is not physically viable, surface diffusion was established as the rate-determining process in intra-particle mass transfer. Mass transfer across the stagnant solution film surrounding the carbon particle, and surface diffusion into the carbon particle, are thus the rate-determining mechanisms in most instances in which gold di-cyanide is adsorbed onto activated carbon.

Acknowledgements

Support by Gencor Pty Ltd is gratefully acknowledged. Dr P.C. Pistorius is thanked for his interest and helpful comments.

References

1. Dixon, S., Cho, E.H., and Pitt, C.H. The interaction of gold cyanide, silver cyanide and high surface area charcoal. *AIChE Symp. Series,* vol. 174, no. 173. 1976. pp. 75–83.
2. Cho, E.H., Dixon, S.N., and Pitt, C.H. The kinetics of gold cyanide adsorption on activated charcoal. *Metall. Trans. B,* vol. 10B. 1979. pp. 185–189.
3. Fleming, C.A., and Nicol, M.J. The adsorption of gold cyanide onto activated carbon. III. Factors influencing the rate of loading and the equilibrium capacity. *J. S. Afr. Inst. Min. Metall.,* vol. 84, no. 4. 1984. pp. 85–93.
4. Fuerstenau, M.C., Nebo, C.O., Kelso, J.R., and Zaragoza, R.M. Rate of adsorption of gold cyanide on activated charcoal. *Minerals and Metallurgical Processing,* vol. 4 no. 4. 1987. pp. 177–181.
5. Zarrouki, M., and Thomas, G. Etude de l'adsorption de complexes cyanurés sur charbon actif. *J. Chim. Phys.,* vol. 87. 1990. pp. 1715–1762.
6. Cho, E.H., and Pitt, C.H. Kinetics and thermodynamics of silver cyanide adsorption on activated charcoal. *Metall. Trans. B,* vol. 10B. 1979. pp. 165–169.
7. Van Deventer, J.S.J. Kinetic models for the adsorption of gold onto activated carbon. *MINTEK 50. Proceedings International Conference on Mineral Science and Technology.* Haughton, L.F. (ed.). Randburg, (South Africa), Council for Mineral Technology, 1984. pp. 487–494.
8. Van Deventer, J.S.J. Kinetic model for the reversible adsorption of gold cyanide on activated carbon. *Chem. Eng. Comm.,* vol. 44. 1986. pp. 257–274.
9. Jones, W.G., and Linge, H.G. Effect of ore pulp on the adsorption rate of gold cyanide on activated carbon. *Hydrometallurgy,* vol. 22. 1989. pp. 231–238.
10. McDougall, G.J., Hancock, R.D., Nicol, M.J., Wellington, O.L., and Copperthwaite, R.G. The mechanism of the adsorption of gold cyanide onto activated carbon. *J. S. Afr. Inst. Min. Metall.,* vol. 80, no. 9. 1980. pp. 344–356.
11. Yapu, W., Segarra, M., Fernández, M., and Espiell, F. Adsorption kinetics of dicyanoaurate and dicyanoargentate ions in activated carbon. *Metall. Trans. B,* vol. 25B. 1994. pp. 185–191.
12. Jordi, R.G., Young, B.D., and Bryson, A.W. Gold adsorption on activated carbon and the effect of suspended solids and dissolved silicon dioxide. *Chem. Eng. Comm.,* vol. 102. 1991. pp. 127–147.
13. Vegter, N.M. The distribution of gold in activated carbon during adsorption from cyanide solutions. *Hydrometallurgy,* vol. 30. 1992. pp. 229–242.
14. Carrier, C., Hodouin, D., and Courchesne, M. Dynamic simulation of the CIP gold recovery process. *Proceedings of the International Symposium on Gold Metallurgy.* Salter, R.S., Wyslouzil, D.M., and McDonald, G.W. (eds.). Winnipeg (Canada), CIM, 1987. pp. 309–325.
15. Stange, W., King, R.P., and Woollacott, L. Towards more effective simulation of CIP and CIL processes. 2. A population-balance-based simulation approach. *J. S. Afr. Inst. Min. Metall.,* vol. 90, no. 11. 1990. pp. 307–314.
16. Woollacott, L.C., Stange, W., and King, R.P. Towards more effective simulation of CIP and CIL processes. 1. The modelling of adsorption and leaching. *J. S. Afr. Inst. Min. Metall.,* vol. 90, no. 10. 1990. pp. 275–282.
17. Nicol, M.J., Fleming, C.A., and Cromberge, G. The absorption of gold cyanide onto activated carbon. I. The kinetics of adsorption from pulps. *J. S. Afr. Inst. Min. Metall.,* vol. 84, no. 2. 1984. pp. 50–54.

18. JOHNS, M.W. The simulation of gold adsorption by carbon using a film diffusion model. Johannesburg (South Africa), University of the Witwatersrand, M.Sc. dissertation, 1987.
19. LE ROUX, J.D., BRYSON, A.W., and YOUNG, B.D. A comparison of several kinetic models for the adsorption of gold cyanide onto activated carbon. *J. S. Afr. Inst. Min. Metall.*, vol. 91, no. 3. 1991. pp. 95–103.
20. PETERSON, F.W., and VAN DEVENTER, J.S.J. Inhibition of mass transfer to porous adsorbents by fine particles and organics. *Chem. Eng. Comm.*, vol. 99. 1991. pp. 55–75.
21. PETERSON, F.W., and VAN DEVENTER, J.S.J. The influence of pH, dissolved oxygen and organics on the adsorption of metal cyanides on activated carbon. *Chem. Eng. Sci.*, vol. 46, no. 12. 1991. pp. 3053–3065.
22. YOUNG, B.D., LE ROUX, J.D., and BRYSON, A.W. The binary adsorption of gold cyanide and ethyl xanthate onto activated carbon. *Hydrometallurgy*, vol. 26, no. 3. 1991. pp. 395–401.
23. AHMED, F.E., YOUNG, B.D., and BRYSON, A.W. Comparison and modelling of the adsorption kinetics of gold cyanide onto activated carbon and resin in a silica slurry. *Hydrometallurgy*, vol. 30. 1992. pp. 257–275.
24. PETERSON, F.W., and VAN DEVENTER, J.S.J. The interaction between organics and metal complexes in adsorption columns. *Minerals Engineering*, vol. 5, no. 1. 1992. pp. 1–16.
25. OTU, E.O., BYERLEY, J.J., and ROBINSON, C.W. Kinetic modelling of gold cyanide multi-cycle adsorption and elution using activated carbon in the presence of foulants. *Can. J. Chem. Eng.*, vol. 71. 1993. pp. 925–933.
26. NAG. *Fortran library*. Oxford, (UK).
27. IMSL. *Math/library user's manual*. Version 1.1. Houston (USA), 1989. pp. 409–411, 434–435, 872–875.
28. VAN DER MERWE, P.F. Fundamentals of the elution of gold cyanide from activated carbon. Stellenbosch (South Africa), University of Stellenbosch, Ph.D. dissertation, 1991. pp. 92, 405, 407, 409, 411.
29. VAN DEVENTER, J.S.J. Kinetic model for the adsorption of metal cyanides on activated charcoal. Stellenbosch (South Africa), University of Stellenbosch, Ph.D. dissertation, 1984. pp. 114–115, 132, 139.
30. LE ROUX, J.D. Modelling of the effect of organic fouling on the adsorption of gold cyanide by activated carbon in a batch reactor. Johannesburg (South Africa), University of the Witwatersrand, M.Sc. dissertation, 1989. pp. 130, 170, 174–175.
31. VAN LIER, W.C. Mass transfer to activated carbon in aqueous solutions. Delft (Netherlands), Technical University of Delft, Ph.D. dissertation, 1989. p. 81.
32. LEYVA-RAMOS, R., and GEANKOPLIS, C.J. Diffusion in liquid-filled pores of activated carbon. I. Pore volume diffusion. *Can. J. Chem. Eng.*, vol. 72. 1994. pp. 262–271.
33. CHEH, H.Y. Electrodeposition of gold by pulsed current. *J. Electrochem. Soc.*, vol. 118, no. 4. 1971. pp. 551–557.
34. MACARTHUR, D.M. A study of gold reduction and oxidation in aqueous solutions. *J. Electrochem. Soc.*, vol. 119, no. 6. 1972. pp. 672–677
35. NICOL, M.J., SCHALCH, E., and BALESTRA, P. A modern study of the kinetics and mechanism of the cementation of gold. *J. S. Afr. Inst. Min. Metall.*, vol. 79, no. 2. 1979. pp. 191–198.
36. RUBCUMINTARA, T., and HAN, K.N. The effect of concentration and temperature on diffusivity of metal compounds. *Metall. Trans. B.*, vol. 21B. 1990. pp. 429–438.
37. HARRIOT, P. Mass transfer to particles: Part 1. Suspended in agitated tanks. *AIChE J.*, vol. 8, no. 1. 1962. pp. 93–102.

List of symbols

b = exponent of the Freundlich isotherm

B_F = pre-exponential constant of the Freundlich isotherm

B_L = Langmuir constant

Bi_p = modified Biot number (pore diffusion being rate determining)

Bi_s = modified Biot number (surface diffusion being rate determining)

C = gold concentration in pore solution (mg/l)

$\overline{C}$ = mean gold concentration in pore solution (mg/l)

C_b = bulk gold concentration in solution (mg/l)

C_d = change-over concentration in Freundlich and Langmuir isotherms (mg/l)

C_s = gold concentration in solution at the carbon surface (mg/l)

C_{bO} = initial bulk gold concentration in solution (mg/l)

D = molecular diffusivity in solution (m^2/s)

D_p = effective pore diffusivity (m^2/s)

D_s = effective surface diffusivity (m^2/s)

E_s = activation energy of surface diffusion (J/mol)

i = geometric indicator with 1 = cylindrical and 2 = spherical particles

J_f = mass flux across the film ($mg/m^2 \cdot s$)

J_p = mass flux due to pore diffusion ($mg/m^2 \cdot s$)

J_s = mass flux due to surface diffusion ($mg/m^2 \cdot s$)

k_f = constant of film mass-transfer rate (m/s)

K = number of estimated parameters

m = mass of carbon (kg)

n = counter of the number of data points

N = total number of data points

q = gold concentration on the carbon (mg/kg)

$\overline{q}$ = mean gold concentration on the carbon (mg/kg)

q_d = change-over concentration in Freundlich and Langmuir isotherms (mg/kg)

q^* = Langmuir saturation concentration

Q = non-dimensional concentration on the carbon

$\overline{Q}$ = non-dimensional mean concentration on the carbon

r_s = radius of the carbon particle (m)

t = time (s)

V = solution volume (m^3)

α = non-dimensional parameter

ζ = non-dimensional concentration in solution

ζ_b = non-dimensional bulk concentration in solution

ζ_d = non-dimensional dilute isotherm change-over concentration in solution

ε_p = porosity of carbon particle

ρ_p = apparent density of carbon particle (kg/m^3)

τ_m = tortuosity

τ_p = non-dimensional time

τ_s = non-dimensional time ◆